AIAA JOURNAL
Vol. 42, No. 7, July 2004

Residual Stress Creep Relaxation Around Cold Expanded Holes in an Aluminum Alloy

V. Lacarac,* D. J. Smith,† and M. J. Pavier‡
University of Bristol, Bristol, England BS8 1TR, United Kingdom

Residual stress distributions were measured in aluminum-alloy 2650 disks after cold expansion and after exposure to creep at 150°C for various times. Strains measured as a result of boring out the hole after cold expansion were found to exhibit significant angular variations around the hole. However, after exposure to 150°C residual strains and stresses showed less angular variation. To take account of the angular variation, the Garcia–Sachs technique for measuring residual stresses was employed. Surface residual stresses on the entrance and exit faces of the disks were measured using the x-ray method. The most significant relaxation of the residual stresses occurred within the first 100 h. Two simple models were used to predict residual stress relaxation, one using a uniaxial creep relaxation model and a second using tensile and isochronous stress–strain curves. A good comparison between predictions and experiments was observed.

I. Introduction

COLD expansion is a manufacturing process for introducing compressive residual stresses in material surrounding a hole. This process is used in age-hardened 2000 and 7000 series of aluminum alloys to enhance their fatigue life. However, cold expansion is not extensively used for higher operating temperatures because the residual stresses are thought to be relieved by creep. This is particularly relevant for proposed advanced supersonic transport required to fly at Mach 2.4 (Ref. 1), where the skin temperature is expected to be as high as 150°C.

Earlier work has shown that relaxation of residual stress occurs when components are subjected to elevated temperature. For example, Throop[2] examined relaxation of autofrettaged residual stresses in thick-walled tubes. For residual stresses arising from cold expansion, Fowler[3] observed that the benefit of cold expansion can be retained depending on the applied temperature and loading conditions. Nevertheless, results for the residual stress relaxation around cold-expanded holes are very limited. The purpose of this paper is to examine the nature of the residual stress redistribution around cold-expanded holes in an aluminum alloy.

It has been recently shown[4–8] that cold expansion using a split sleeve introduces a complex three-dimensional residual stress field. To determine such a residual stress field, a number of measurement techniques are required. For example, the x-ray technique[9] and the Garcia–Sachs method[10] have been used to determine surface and average through-thickness residual stresses around cold-expanded holes. Unlike the conventional Sachs method,[11] the Garcia–Sachs method was able to measure the residual stress variation[4,5] around the hole. These results also demonstrated good agreement with the results obtained using the x-ray method and with results from finite element simulations.[4,5]

In this paper, new results using the Garcia–Sachs and x-ray method are reported for nonaxisymmetric residual stresses around cold-expanded holes in disks of aluminum alloy 2650. Disks were then subjected to a high temperature (150°C) for different duration, and the residual stresses measured. It is shown that relaxation and redistribution of the initial residual stresses occurred, with the majority of relaxation taking place in the first 100 h. Relaxation of the residual stresses is then predicted using two novel one-dimensional methods, and predictions are compared with experimental results. It is also demonstrated that complete relaxation does not occur.

Received 31 May 2001; revision received 30 November 2003; accepted for publication 5 February 2004.

*Research Assistant, Department of Mechanical Engineering.
†Professor, Department of Mechanical Engineering.
‡Reader, Department of Mechanical Engineering.

II. Experiments

A. Material and Specimens

The material used was aluminum alloy Al 2650, with the chemical composition as follows: 94.55% Al, 2.76% Cu, 1.74%Mg, 0.34%Mn, 0.41%Si, 0.11%Fe, 0.09%Ti. The yield stress and tensile strength are 430 and 460 MPa, respectively, Young's modulus 72 GPa, and Poisson's ratio 0.33.

Five disks with a 32-mm outside diameter, 6 mm thick and containing a central hole of diameter 6 mm, were extracted from 25-mm-thick Al 2650 plate. The disks were then subjected to nominal 4% cold expansion using the split-sleeve process developed by Fatigue Technology Incorporated. The location of the split in the sleeve during cold expansion is defined as $\theta = 0$ deg, as shown in Fig. 1. The cold-expanded holes were then reamed to remove extraneous material generated at the location of the split in the sleeve. Disk 1 was used for residual stress measurement after cold expansion. Disks 2–5 were placed in a furnace and subjected to 150°C for various times. A summary of all of the test conditions are shown in Table 1. All disks were examined using the x-ray and the Garcia–Sachs methods to obtain residual stress distributions.

B. Experimental Methods

Strain gauges were bonded at the periphery of the disks to measure strain relaxation using the Garcia–Sachs method. Six strain gauges in the hoop direction were bonded at $\theta = 0$, 45, 90, 135, 180, and 270 deg on the edge of the disks, as shown in Fig. 1. The strain gauges at $\theta = 90$ and 270 deg were used to check symmetry conditions. In each disk the center hole was then bored out incrementally. A sharp tool, a slow cutting speed, and a feed rate of 1 mm/s with copious amounts of coolant were employed to minimize the possibility of generating further residual stresses in the exposed surface during metal removal. Cuts were made in radial increments of about 0.05 mm and strain readings taken typically every 0.2 mm increasing to 0.5 mm for a radial distance greater than 6 mm from the hole edge. A micrometer was used to measure the hole diameter corresponding to each strain reading.

X-ray residual stress measurements were made using a Siemens D500 diffractometer using CuK_α radiation at 40 kV and 40 mA. Data collection times were reduced by using a position sensitive detector. The peak occurring at 139.5 deg (2θ) diffracting from the {422} planes was used for stress measurement. The x-ray beam was collimated to give an irradiated area of about 1×1 mm, and

a computer program was used to interpret the diffraction data. The analysis assumed a biaxial stress state and employed the $\sin^2\psi$ technique[12] in the calculation of stress. $\mathrm{Sin}^2\psi$ values were chosen in the range 0.0–0.5.

X-ray measurements were made on the entrance and exit faces of the disks. Two angular positions were examined, $\theta = 0$ and $\theta = 90$ deg. At each angle, measurements were made at different radial locations, starting at the edge of the central hole and moving toward the edge of the disk.

C. Results

1. Garcia–Sachs Method

In the Garcia–Sachs method the residual stresses are calculated from the measured strains on the periphery of the disk. First, a Fourier analysis of the hoop strains $\varepsilon_{\theta\theta}(r,\theta)$ was performed using

$$\varepsilon_{\theta\theta}(r,\theta) = \sum_{n=0}^{4} \varepsilon_{\theta\theta}^{(nc)}(r)\cos(n\theta) \tag{1}$$

where r and θ are defined in Fig. 1 and $\varepsilon_{\theta\theta}^{(nc)}$ are the Fourier coefficients. The analysis of hoop strains was restricted to the first five Fourier terms ($n = 0$ to 4), and the coefficients $\varepsilon_{\theta\theta}^{(nc)}$ in Eq. (1) were calculated. Further details of the Garcia–Sachs method are presented elsewhere.[6,10] The results for hoop strains at 270 deg were essentially identical in magnitude to those at 90 deg, showing that there was symmetry of the strains.

The Fourier coefficients are shown in Fig. 2 for the two conditions, immediately after cold expansion and after creep for 1000 h. Only the first three Fourier terms are shown because the magnitudes of the higher-order terms are relatively small. The zero Fourier term $\varepsilon_{\theta\theta}^{0}$ is most significant and represents a symmetrical component of relaxed hoop strain.

Higher-order terms indicate the presence of nonaxisymmetric stress–strain fields. The term $\varepsilon_{\theta\theta}^{1}$ is larger than $\varepsilon_{\theta\theta}^{2}$, thus indicating a perturbation in the residual stress field located at $\theta = 0$ deg, that is, at the pip. After creep for 1000 h, marked reductions in higher-order terms were observed for disk 5, indicating a lower level of nonaxisymmetricity of the residual strain field compared to the initial cold-expanded condition.

Measured hoop strain distributions around a cold-expanded hole for different exposure times are shown in Fig. 3. The strain distributions are at 0.96 mm from the hole edge (that is $r/r_a = 1.3$). It is evident that the hoop strain decreased over time. The major change in hoop strain took place during the first 100 h with exposure to longer times producing only a small additional strain relaxation. Similar strain relaxation was measured at $\theta = 0$ and 90 deg, whereas at 180 deg there was hardly any change in strains as a function of time.

Table 1 Summary of test conditions

Disk number	Condition
1	Only cold expanded
2	Exposure at 150°C for 10 h
3	Exposure at 150°C for 100 h
4	Exposure at 150°C for 300 h
5	Exposure at 150°C for 1000 h

Equation (1) decomposes the strain distributions into Fourier coefficients. To obtain the residual stress for each Fourier coefficient, the method developed by García-Granada et al.[10] was used. In general, the Fourier coefficients of the hoop $\sigma_{\theta\theta}^{(nc)}$, radial $\sigma_{rr}^{(nc)}$, and shear $\tau_{r\theta}^{(nc)}$ residual stresses are given by

$$\sigma_{\theta\theta}^{(nc)} = \sigma_{rr}^{(nc)} + r\frac{\partial\sigma_{rr}^{(nc)}}{\partial r} + n\tau_{r\theta}^{(nc)}$$

$$\sigma_{rr}^{(nc)} = -Ef(n,r)\left[\varepsilon_{\theta\theta}^{(nc)} - g_1(n,r)\int_a^r h(n,r')\varepsilon_{\theta\theta}^{(nc)}\partial r'\right]$$

$$\tau_{r\theta}^{(nc)} = -nEf(n,r)\left[\varepsilon_{\theta\theta}^{(nc)} - g_2(n,r)\int_a^r h(n,r')\varepsilon^{(nc)}\partial r'\right] \tag{2}$$

where E is Young's modulus; n is the coefficient number ($n = 1, 2, ..$); and $f(n,r)$, $g_1(n,r)$, $g_2(n,r)$, and $h(n,r')$ are

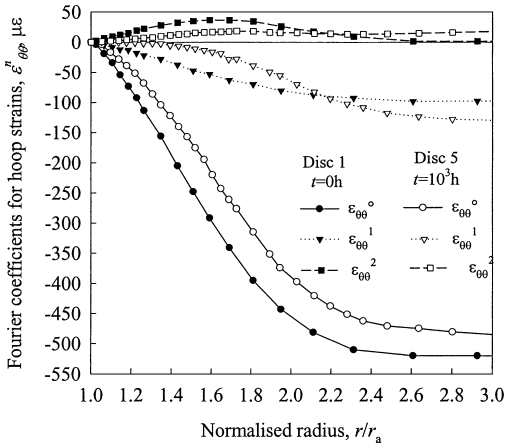

Fig. 2 Comparison of Fourier coefficients for hoop strains after cold expansion and after exposure at 150°C for 1000 h.

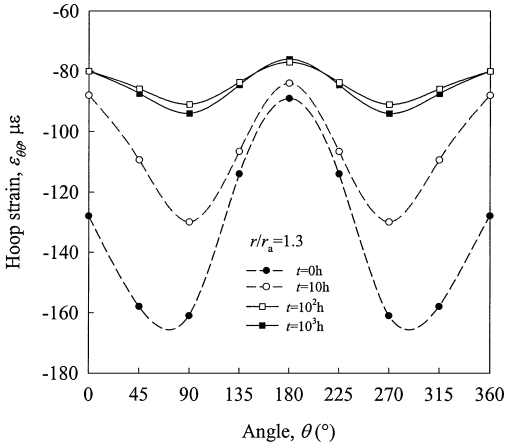

Fig. 3 Measured hoop strains.

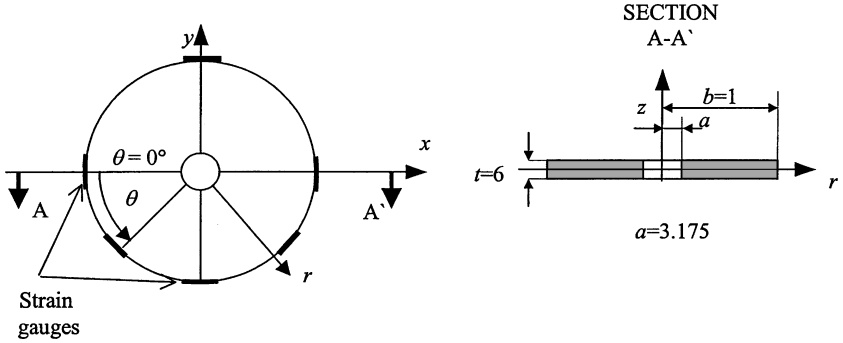

Fig. 1 Dimensions of disks used in residual stress measurements. All dimensions in millimeters.

functions. Examples of the functions are given by Ref. 6. Finally, the complete hoop residual stress distribution $\sigma_{\theta\theta}(r, \theta)$ was determined by summing the coefficients, where

$$\sigma_{\theta\theta}(r, \theta) = \sum_{n=0}^{\infty} \sigma_{\theta\theta}^{(nc)}(r) \cos(n\theta) \tag{3}$$

Similar methods were used for the radial $\sigma_{rr}(r, \theta)$ and shear $\tau_{r\theta}(r, \theta)$ residual stress distribution. The measured hoop residual stresses for various exposure times are shown in Fig. 4, with Figs. 4a and 4b showing results at $\theta = 0$ and 90 deg, respectively. Typical errors

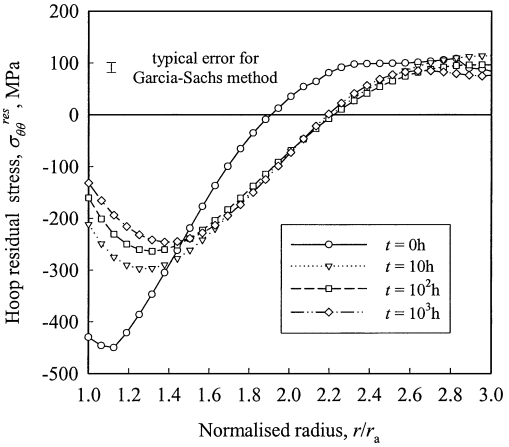

Fig. 4a Hoop residual stresses measured using the Garcia–Sachs method at $\theta = 0$ deg.

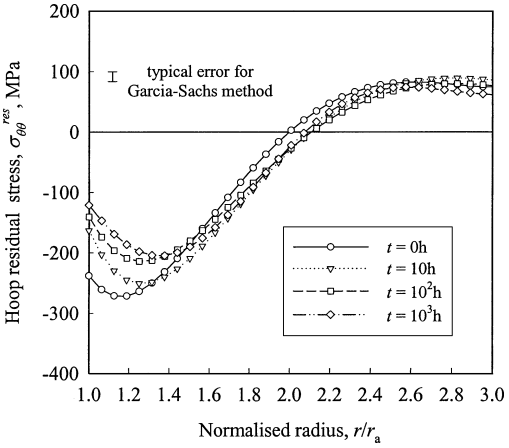

Fig. 4b Hoop residual stresses measured using the Garcia–Sachs method at $\theta = 90$ deg.

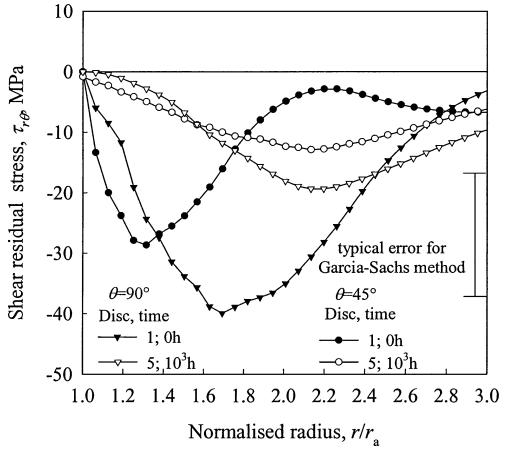

Fig. 4c Shear residual stress measured using the Garcia–Sachs method at $\theta = 90$ and 45 deg.

for the measured residual stress using the Garcia–Sachs have been shown to be about 20 MPa (Ref. 5). It can be seen that major relaxation of the hoop stress takes place in the first 100 h. Between 100 and 1000 h there was little change in the residual stress distribution. The stress distribution changed in such a way that the compressive residual stresses became less compressive, and the tensile stresses became less tensile. The greatest amount of relaxation of the residual stresses took place at $\theta = 0$ deg, as shown in Fig. 4a. For example, the maximum hoop stresses relaxed by approximately 180 MPa at $\theta = 0$ deg, whereas at $\theta = 90$ deg the residual stresses shown in Fig. 4b relaxed by about 70 MPa. Also, as a result of relaxation, the location of maximum compressive stress at $\theta = 0$ deg shifted from $r/r_a = 1.1$ to 1.4.

The shear residual stresses in the initial cold expanded condition and after 1000 h are shown in Fig. 4c. The magnitude of the shear stress was small. Nevertheless, the results show that the shear residual stresses redistributed, by approximately 30 and 25 MPa at angular positions $\theta = 90$ and 45 deg, respectively.

2. *X-Ray Method*

The results from the Garcia–Sachs method represent the average through-thickness residual stresses as a function of radial and angular position. In contrast, the x-ray method measured the near-surface residual stresses on the entrance and exit faces of the cold-expanded disks. The method of cold expansion used here produces a variation of residual stress through the thickness. Therefore it is expected that the Garcia–Sachs and x-ray results will be different.

The x-ray results at the entrance and exit faces for disks 1 and 5 ($t = 0$ and 1000 h) at $\theta = 0$ and 90 deg are shown in Fig. 5 and compared with the Garcia–Sachs results. Results at $\theta = 0$ deg, on the entrance and exit faces are shown in Figs. 5a and 5b, and a set for $\theta = 90$ deg is shown in Figs. 5c and 5d. The x-ray measurements at $\theta = 0$ and 90 deg and at the entrance and exit faces illustrate that there was a through-thickness distribution of residual stress after cold expansion. For example, the residual stress at the entrance face was lower than at the exit face. There was also an angular variation in surface residual stresses, with larger surface residual stresses at $\theta = 0$ than at 90 deg. The least compressive residual stress occurred at $\theta = 90$ deg on the entrance face of the cold-expanded aluminum disks.

After exposure at 150°C for 1000 h, the results in Fig. 5 show that in general the surface residual stresses relax, just for the average through-thickness stresses. It is evident that a more pronounced relaxation occurred at the exit face compared to the entrance face. This is because the compressive residual stresses were larger at the exit face. For example, at $\theta = 0$ deg at the exit and entrance face, the hoop residual stresses had relaxed by 100 and 70 MPa, respectively. On the other hand, at $\theta = 90$ deg on the entrance face, stress relaxation was not observed. With this exception, at the other measurement locations Figs. 5a–5d reveal that the surface measurements using the x-ray method, essentially matched the measurements obtained from the Garcia–Sachs method.

The measured peak compressive hoop stresses obtained using the Garcia–Sachs and x-ray method are summarized in Fig. 6. Overall, the measurements demonstrate that the majority of residual stress relaxation occurred in the first 100 h. Both methods also revealed that the residual stress distribution became more symmetric during the relaxation process. Nevertheless, the largest compressive residual stress occurred at $\theta = 0$ deg, with the smallest at 180 deg. The rate of stress relaxation was dependent on the magnitude of the residual stresses: the larger the stress the larger the relaxation. The results show that at $\theta = 90$ and 0 deg relaxation was more significant than at $\theta = 180$ deg.

III. Prediction of Stress Relaxation

In general, the operating conditions for any component vary over a wide range, and it is not practical to undertake residual stress measurements for all conditions. Therefore, it is important to be able to predict the extent of residual stress relaxation. Predictions are made using two methods, one based on a simple uniaxial model of the relaxation of the hoop residual stress and the second using

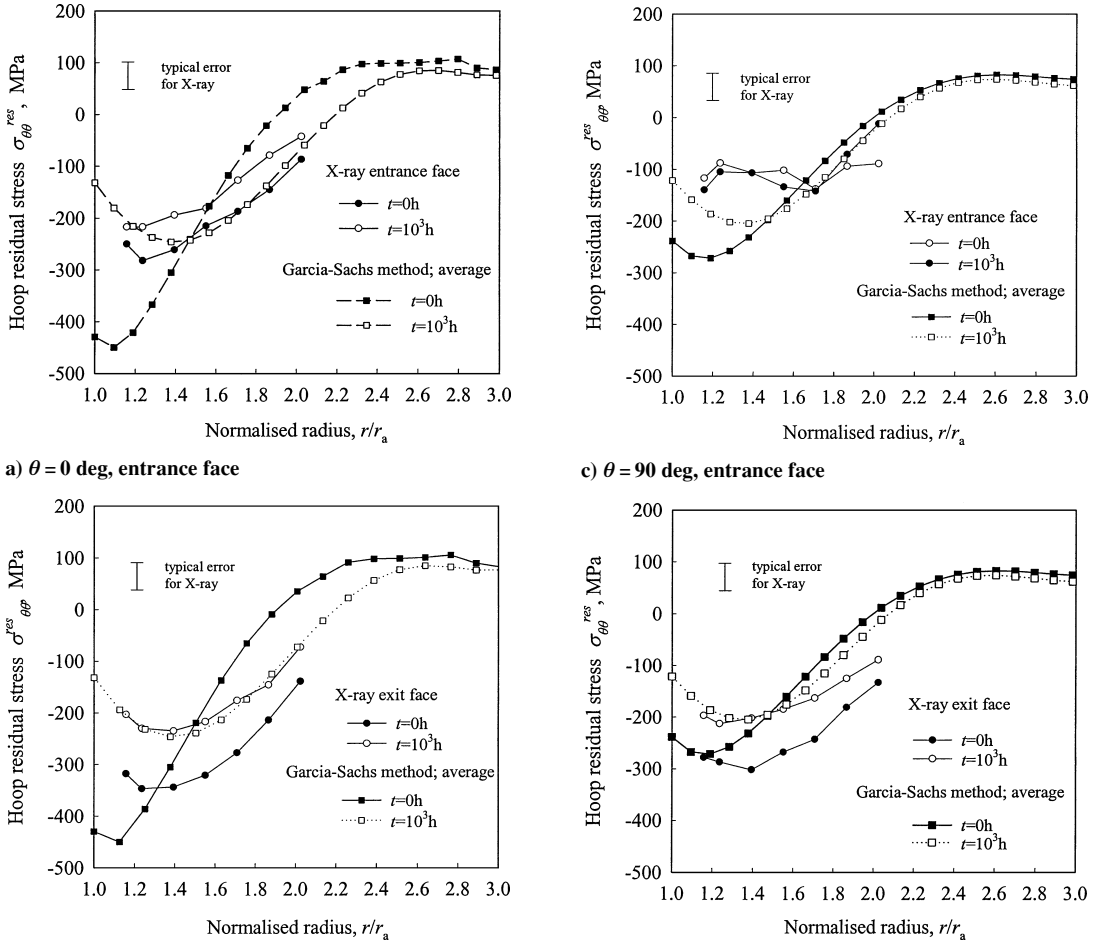

a) $\theta = 0$ deg, entrance face

c) $\theta = 90$ deg, entrance face

b) $\theta = 0$ deg, exit face

d) $\theta = 90$ deg, exit face

Fig. 5 Measured hoop residual stresses around a cold-expanded hole, before and after creep relaxation.

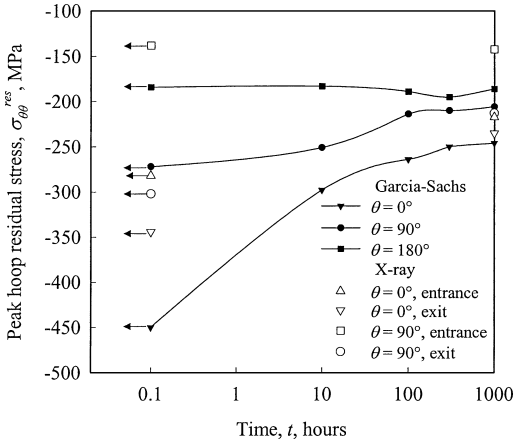

Fig. 6 Residual stress relaxation at 150°C.

the maximum equivalent residual stress together with isochronous stress–strain curves to estimate the relaxation of residual stress.

A. Simple Uniaxial Model

In this model it is assumed that the relaxation process occurs under constant total strain ε_T, which here is the sum of the elastic ε_e and creep strains ε_c, where

$$\varepsilon_e + \varepsilon_c = \varepsilon_T \tag{4}$$

The elastic and creep strains are given by

$$\varepsilon_e = \sigma/E, \qquad \varepsilon_c = B\sigma^n t^m \tag{5}$$

where σ is stress; t is time; E is Young's modulus; and B, n, and m are material constants used to describe the primary creep behavior of the aluminum alloy.

Differentiating Eq. (4) and rearranging gives

$$\frac{1}{E}\frac{\partial \sigma}{\partial t} = -Bm\sigma^n t^{m-1} \tag{6}$$

Separating the variables σ and t, and integrating Eq. (6) yields

$$\int_{\sigma_0}^{\sigma} \frac{\mathrm{d}\sigma'}{\sigma^n} = -EBm \int_0^t t^{m-1}\,\mathrm{d}t' \tag{7}$$

where is σ_0 the initial applied stress.

The solution to Eq. (7) is

$$\sigma = \left[\sigma_0^{1-n} + (n-1)BEt^m\right]^{1/(1-n)} \tag{8}$$

Equation (8) describes the relaxation of initial applied stress for a uniaxial bar subjected to constant displacement. For a multiaxial stress state the uniaxial stress can be replaced by an effective or equivalent stress. This uniaxial model was used to predict the relaxation of the magnitude of the maximum compressive hoop residual stress irrespective of angular location. Using this prediction at a given time, the ratio of the relaxed peak hoop residual stress to the initial peak hoop residual stress was determined. The distribution of the hoop residual stresses at other radial locations was determined using this ratio. At a given time t,

$$\frac{\sigma_{\theta\theta}(t)}{\sigma_{\theta\theta}|_{t=0}} = \frac{\sigma_{\theta\theta,\max}(t)}{\sigma_{\theta\theta,\max}|_{t=0}} \tag{9}$$

The creep material constants in Eq. (8) for aluminum 2650 at 150°C were obtained from a series of uniaxial creep tests for a range of stress and temperatures of interest. The details of the tests are

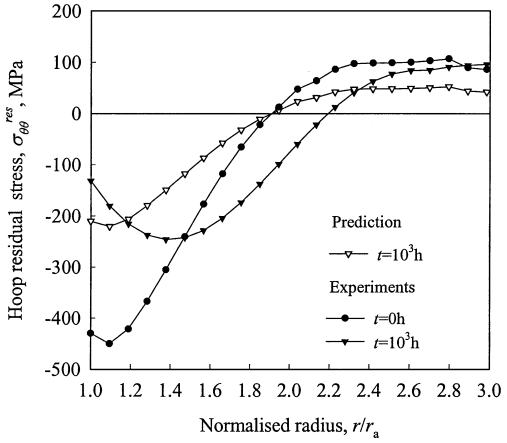

a) $\theta = 0$ deg

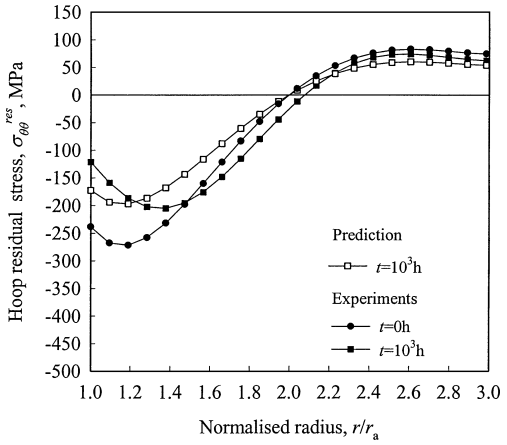

b) $\theta = 90$ deg

Fig. 7 Comparison between predicted and Garcia–Sachs measured hoop residual stress distribution.

described by García-Granada.[6] The material constants are $m = 0.32$, $n = 7.5$, and $B = 1.15 \times 10^{-23}$ MPa^{-n}s^{-m}.

Predictions for the relaxed hoop residual stress were obtained for different times using Eq. (8) combined with Eq. (9). Results for the predicted hoop residual stress distribution after 1000 h relaxation are shown in Fig. 7. The results are compared with Garcia–Sachs measurements including the initial residual stress distribution. There is good agreement between the prediction and the experimental measurements at $\theta = 90$ deg although at $\theta = 0$ deg the predicted distribution is rather poor. The maximum discrepancy between predicted and measured residual stresses at $\theta = 90$ deg was 50 MPa. Bearing in mind that the standard deviation in residual stress measurements was approximately 20 MPa (Ref. 5) and that a very simple model was used, this level of agreement is expected. In addition, the scatter in the hoop residual stresses for a similar nominal cold expansion was reported to be 50 MPa (Refs. 5 and 9). This scatter might also affect the level of discrepancy between predictions and measurements.

The predictions of the relaxation of peak compressive hoop stress are summarized and compared to measured residual stresses in Fig. 8. The predictions show similar trends to the experimental results, with the predictions generally overestimating the relaxation of the peak hoop stress.

B. Relaxation of Equivalent Stress

Measurements of the residual stresses revealed that cold expansion introduces a three-dimensional stress field around a hole. The simple uniaxial model can also be used to describe the relaxation of equivalent stress. Alternatively it is instructive to examine relaxation of an equivalent stress using isochronous stress–strain curves.

At any given time the total strain is the sum of the elastic, plastic, and creep strains. The stress–strain curves from tensile tests at 20°C and 150°C (Refs. 5 and 6) are shown in Fig. 9. Also shown are isochronous stress–strain curves calculated using Eq. (2). It can be seen that for times less than 1000 h there is very little creep deformation below 200 MPa. At higher stresses the isochronous stress–strain curves lie below the tensile curve at 150°C.

Equivalent residual stresses were calculated from the measured residual stress at all radial locations and a given angular location using

$$\sigma_{\text{eq}} = \sqrt{\left((\sigma_{\theta\theta} - \sigma_{\text{rr}})^2 + \sigma_{\text{rr}}^2 + \sigma_{\theta\theta}^2 + \sigma_{r\theta}^2\right)/2} \qquad (10)$$

The peak equivalent residual stresses are shown in Fig. 10 for angular locations at $\theta = 0$, 90, and 180 deg. Also shown in Fig. 10 are predictions of the relaxation of the equivalent stresses using the curves shown in Fig. 9. To determine the degree of relaxation, it is

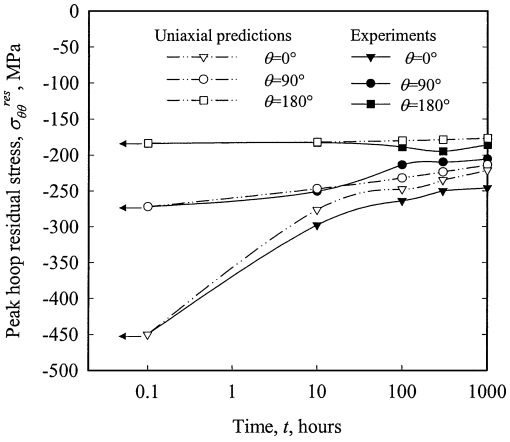

Fig. 8 Residual stress relaxation at 150°C.

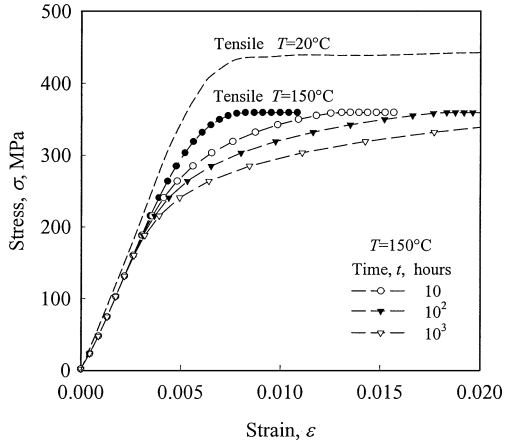

Fig. 9 Isochronous stress–strain curves for aluminum alloy 2650.

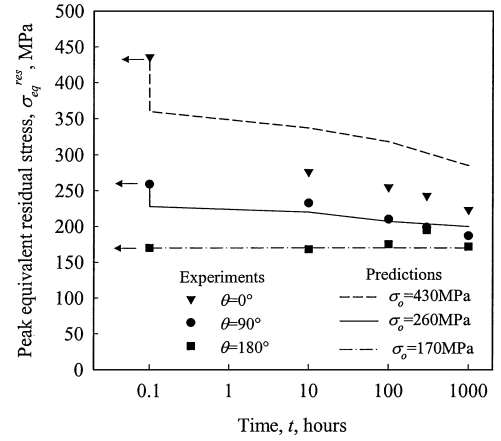

Fig. 10 Comparison between predictions and Garcia–Sachs measurements.

assumed that relaxation occurred at constant total strain, with the initial equivalent stress corresponding to the measured stress after cold expansion. For example, the peak initial equivalent residual stress at $\theta = 90$ deg was 270 MPa, corresponding to a total strain of 0.42%. After 1000 h at 0.42%, total strain, the equivalent stress from Fig. 9 is 220 MPa. Relaxation of the equivalent stress at other angular locations and different times was also calculated using this analysis. For high initial equivalent residual stresses, the tensile and isochronous stress–strain curves illustrate that instantaneous relaxation of the stress occurs as a result of the decrease in the stress to cause plasticity at a higher temperature. Further relaxation then takes place from time-dependent (creep) deformation.

IV. Discussion

Immediately after cold expansion there was a significant difference in the residual stresses on the entrance and exit faces, with residual stresses on the exit face being more compressive (Figs. 5b–5d). The difference between the exit and entrance faces was more pronounced at an angle of 90 deg compared to 0 deg. For example the largest difference between the two faces was 200 and 100 MPa at 90 and 0 deg, respectively. The residual hoop stresses also varied as a function of position around the periphery of the hole, and they were more compressive at 0 deg. Depending on radial distance from the hole edge, the magnitude of the surface hoop residual stress at $\theta = 90$ deg was lower compared to $\theta = 0$ deg.

The results shown in Figs. 2 and 3 demonstrate that the initial nonaxisymmetric strain field, generated through cold expansion of the hole, was not retained after exposure to 150°C for 1000 h. The measured angular hoop strain distribution shown in Fig. 3 revealed that the residual stress field became more uniform with increasing time. For example, by comparing results at $\theta = 0$ and 90 deg (Fig. 4) the residual stress distributions after 1000 h (disk 5) at the hole edge and for $r/r_a > 2.4$ are relatively axisymmetric.

Nevertheless, for $1.2 < r/r_a < 2.4$ a nonaxisymmetric residual stress field was observed. This degree of nonaxisymmetricity would be likely to remain even for longer exposure times because of the relatively low level of residual stresses.

The experiments revealed that residual stress relaxation through the thickness proceeded in such a way as to generate a more uniform residual stress distribution. For example, the differences between surface hoop residual stresses, after exposure to 150°C, on the exit and entrance faces at $\theta = 0$ and 90 deg had decreased from 110 to 50 MPa and from 200 to 100 MPa, respectively. This level of nonuniform residual stress distribution through the thickness was likely to remain very much the same, even after exposure to longer times. This is because creep deformation was negligible for stresses below 200 MPa.

There are a number of features that influence the relaxation and redistribution of the initial residual stresses. Increasing the temperature lowered the yield stress and introduced time-dependent (creep) deformation. If the residual stress was sufficiently high, stress relaxation occurred as a result of further plasticity and creep. Furthermore the residual stresses redistributed in order to maintain equilibrium. The degree of multiaxiality also influenced the extent of relaxation. For example, no relaxation takes place in situations where the equivalent stress is low, that is, in the presence of hydrostatic residual stresses alone.

The influence of both plasticity and creep was evident in the relaxation of the residual stress at $\theta = 0$ deg compared to other angles around the hole. Residual stresses at $\theta = 0$ deg were on the yield surface, so that exposure to 150°C caused immediate redistribution through plastic deformation, followed by creep deformation.[5] This is evident in Fig. 10, where the initial equivalent residual stress relaxed instantaneously from 430 to 360 MPa with the change in temperature from 20 to 150°C. However, the predicted relaxation using the isochronous stress–strain curves was not as great as observed in the experiments.

The reasonable agreement between the predictions and experiments for residual stress relaxation support the use of rather simple models for relaxation of either the peak hoop stress or the maximum equivalent stress. The uniaxial creep model overestimated the relaxation of the peak hoop residual stress, whereas using the tensile and isochronous stress–strain curves underestimated the relaxation of the maximum equivalent stress. In either case the degree of error between experiment and prediction was not large. Also both models confirm that at 150°C for aluminum alloy 2650 the magnitude of residual stresses does not relax substantially below 200 MPa.

V. Conclusions

Nonaxisymmetric residual stresses were measured for a cold-expanded hole after cold expansion using the Garcia–Sachs and x-ray methods. Significant angular dependence of the residual stresses was demonstrated.

Cold expansion produces a nonuniform through-the-thickness variation of residual stress. Therefore results of the Garcia–Sachs method (which measures averaged through-the-thickness residual stresses) were different from results of the x-ray method (which measures surface residual stresses).

High-temperature exposure at 150°C caused relaxation of residual stresses and led to uniform residual stress distributions through the thickness and around the hole. The degree of relaxation was determined from experimental measurements of residual stresses. It was found that equivalent residual stresses less than about 200 MPa did not relax.

Two simple models were used to predict relaxation, with the predictions being in general agreement with the Garcia–Sachs results.

Acknowledgments

This work was financially supported by a grant from the Department of Trade and Industry (Aerospace Division 4). The support and advice from Phil Holdway and the late Robin Cook at the Defense and Evaluation Research Agency, Farnborough, is gratefully acknowledged.

References

[1]Polmear, I. J., Pons, G., Octor, H., Sanchez, C., Morton, A., Borbridge, W., and Rogers, S., "After Concorde: Evaluation of an Al-Cu-Mg-Ag Alloy for Use in the Proposed European SST," *Aluminium Alloys, Their Physical and Mechanical Properties*, Pts. 1–3, Vols. 217–222, Materials Science Forum, edited by J. H. Driver, B. Dubost, F. Durand, R. Fougeres, P. Guyot, P. Sainfort, and M. Suery, Trans Tech Publications, Zurich, 1996, pp. 1759–1764.

[2]Throop, J. F., "Thermal Relaxation in Autofrettaged Cylinders," *Residual Stress and Stress Relaxation*, edited by E. Kula and V. Weiss, Plenum, New York, 1982, pp. 205–226.

[3]Fowler, R. L., Jr., "Fan Disk Life Extension," U.S. Air Force Materials Lab., Rept. AFWAL-TR-81-4017, Wright–Patterson AFB, Dayton, OH, June 1981.

[4]Garcia-Granada, A. A., Lacarac, V., Holdway, P., Smith, D. J., and Pavier, M. J., "Creep Relaxation of Residual Stresses around Cold Expanded Holes," *Journal of Engineering Materials and Technology*, Vol. 123, No. 1, 2001. pp. 125–131.

[5]Lacarac, V., "Residual Stresses and Fatigue Crack Growth from Cold Expanded Holes in Al2650 at Room and High Temperatures," Ph.D. Dissertation, Dept. of Mechanical Engineering, Univ. of Bristol, Bristol, England, U.K., 2000.

[6]García-Granada, A. A., "The Effect of Creep and Mechanical Load on Cold Expanded Fastener Holes," Ph.D. Dissertation, Dept. of Mechanical Engineering, Univ. of Bristol, Bristol, England, U.K., 2000.

[7]Pavier, M. J., Poussard, C. G. C., and Smith, D. J., "A Finite Element Simulation of the Cold Working Process for Fastener Holes," *Journal of Strain Analysis*, Vol. 32, No. 4, 1997, pp. 287–299.

[8]Hermann, R., "Three-Dimensional Stress Distribution Around Cold Expanded Holes in Aluminium Alloys," *Engineering Fracture Mechanics*, Vol. 48, No. 6, 1994, pp. 819–835.

[9]Cook, R., and Holdway, P., "Residual Stresses Induced by Hole Cold Expansion," *Computer Methods and Experimental Measurements for Surface Treatment Effects*, edited by M. H. Aliabadi and C. A. Brebbia, Computational Mechanics, Southampton, England, U.K., 1993, pp. 91–100.

[10]García-Granada, A. A., Smith, D. J., and Pavier, M. J., "A New Procedure Based on Sachs' Boring for Measuring Non-Axisymmetric Residual Stresses" *International Journal of Mechanical Sciences*, Vol. 42, 2000, pp. 1027–1047.

[11]Sachs, G., "Der Nachweis Innerer Spannungen in Stange und Rohren," *Zitschrift für Metalkunde*, Vol. 19, 1927, pp. 352–357.

[12]Noyan, I. C., and Cohen, J. B., "Residual Stress-Measurement by Diffraction and Interpretation," *MRE*, Springer-Verlag, Berlin, 1987.

A. M. Waas
Associate Editor